Impaired Glutamate Receptor Function Underlies Early Activity Loss of Ipsilesional Motor Cortex after Closed-Head Mild Traumatic Brain Injury

Tyler Nguyen,[1,2] Mohammed Haider Al-Juboori,[3] Jakub Walerstein,[1] Wenhui Xiong,[1] and Xiaoming Jin[1]

Abstract

Although mild traumatic brain injury (mTBI) accounts for the majority of TBI patients, the effects and cellular and molecular mechanisms of mTBI on cortical neural circuits are still not well understood. Given the transient and non-specific functional deficits after mTBI, it is important to understand whether mTBI causes functional deficits of the brain and the underlying mechanism, particularly during the early stage after injury. Here, we used *in vivo* optogenetic motor mapping to determine longitudinal changes in cortical motor map and *in vitro* calcium imaging to study how changes in cortical excitability and calcium signals may contribute to the motor deficits in a closed-head mTBI model. In channelrhodopsin 2 (ChR2)-expressing transgenic mice, we recorded electromyograms (EMGs) from bicep muscles induced by scanning blue laser on the motor cortex. There were significant decreases in the size and response amplitude of motor maps of the injured cortex at 2 h post-mTBI, but an increase in motor map size of the contralateral cortex in 12 h post-mTBI, both of which recovered to baseline level in 24 h. Calcium imaging of cortical slices prepared from green fluorescent calmodulin proteins–expressing transgenic mice showed a lower amplitude, but longer duration, of calcium transients of the injured cortex in 2 h post-mTBI. Blockade of α-amino-3-hydroxy-5-methyl-4-isoxazolepropionic acid or *N*-methyl-D-aspartate receptors resulted in smaller amplitude of calcium transients, suggesting impaired function of both receptor types. Imaging of calcium transients evoked by glutamate uncaging revealed reduced response amplitudes and longer duration in 2, 12, and 24 h after mTBI. Higher percentages of neurons of the injured cortex had a longer latency period after uncaging than that of the uninjured neurons. The results suggest that impaired glutamate neurotransmission contributes to functional deficits of the motor cortex *in vivo*, which supports enhancing glutamate neurotransmission as a potential therapeutic approach for the treatment of mTBI.

Keywords: calcium imaging; controlled cortical impact; neuroplasticity; optogenetic mapping; traumatic brain injury

Introduction

Traumatic brain injury (TBI), as occurs in fallings, sports, and automobile accidents, is a leading cause of death and disability among persons 1–44 years of age.[1] Of all 1.7 million persons who sustain a TBI annually, $\sim 75\%$ of them suffer concussion, a mild form of TBI (mTBI). In contrast to severe TBI that results in skull penetration, hemorrhage, and edema, mTBI patients present with a focal and diffuse injury resulting from non-penetrating head blow. The focal impact is produced by forces acting on the skull that results in local tissue compression beneath the impact site,[2] whereas diffuse impact is produced by a rapid acceleration-deceleration of the head that results in diffuse axonal injury, brain swelling, and hypoxic ischemic damage.[3]

The effects of cellular and molecular perturbations after mTBI are still largely unknown and are sometimes conflicting among different studies. In severe TBI, in addition to impairments including edema, increased intracranial pressure, and hemorrhages, release of excessive glutamate and activation of glutamate receptors are believed to cause intracellular calcium overload, neuronal death, and behavioral deficits.[7,8] Consequently, blocking glutamate receptor activation has generated impetus within the

[1]Indiana Spinal Cord and Brain Injury Research Group, Stark Neuroscience Research Institute and Department of Anatomy, Cell Biology, and Physiology, [2]Medical Neuroscience Program, Stark Neuroscience Research Institute, [3]Indiana Spinal Cord and Brain Injury Research Group, Stark Neuroscience Research Institute and Department of Neurological Surgery, Indiana University School of Medicine, Indianapolis, Indiana, USA.

brain trauma research community and pharmaceutical industry for the treatment of TBI. However, several studies indicate that an increase in synaptic glutamate release may be a transient event, lasting ~8–10 min after mTBI[9] and 30 min after severe TBI.[10]

Further, surface expressions of glutamatergic receptors, including N-methyl-D-aspartate (NMDA) receptors and α-amino-3-hydroxy-5-methyl-4-isoxazolepropionic acid (AMPA) receptors, have been shown to be reduced in many brain areas, especially in motor cortex, whereas activating NMDA receptors, rather than inhibiting them, can improve motor and cognitive behavior of TBI mice in the long term.[11,12] More recent studies demonstrated ineffectiveness or unreliable effectiveness of blocking glutamate receptors as a treatment for TBI in both animal models[14] and human clinical trials.[15] In particular, a phase III clinical study found that treating severe TBI patients with an NMDA receptor antagonist (selfotel) actually resulted in worsening, rather than improving, of the symptoms.[15] Therefore, understanding the time course of cortical functional deficits after brain injury and further examining the role of glutamate excitotoxicity is important to developing effective treatment strategy for mTBI.

Given the transient and non-specific functional deficits after mTBI, there is a lack of insight into the changes in brain function and the underlying mechanism, particularly during the early stage after injury. The recent optogenetic motor mapping technique provides a powerful tool for longitudinally studying dynamic changes of cortical circuits after mTBI.[4–6] Here, for the first time in an mTBI study, we used an *in vivo* optogenetic mapping technique to repeatedly map motor cortex of ChannelRhodopsin 2 (ChR2)-expressing transgenic mice to determine longitudinal changes in cortical motor map after closed-head mTBI. We then imaged calcium signals of spontaneous and glutamate-uncaging evoked activities in brain slices from green fluorescent-calmodulin proteins (GCaMP6) transgenic mice to determine whether dysfunctions of NMDA and AMPA receptors underlay such functional deficits. Our results suggest that reduced functions of these two ionotropic glutamate receptors contributed to the *in vivo* functional deficits observed after mTBI.

Methods

Animals

All animal procedures were approved by the Institutional Animal Care and Use Committee of the Indiana University School of Medicine. Wild-type C57BL/6J (Jax #000664; The Jackson Laboratory, Bar Harbor, ME) mice at 5–7 weeks of age (~20–25 g) were divided into sham and injury groups. For slice-imaging experiments, GCaMP6f (Jax #024276; The Jackson Laboratory, Bar Harbor, ME) transgenic mice at 5–7 weeks of age were divided into multiple groups for different time points after mTBI.

Preparation of mild traumatic brain injury model

mTBI was created using a technique described recently.[16,17] Before injury, mice were anesthetized with a mixture of ketamine (87.7 mg/mL) and xylazine (12.3 mg/mL) and placed in a stereotaxic frame. A heating pad was placed underneath their abdomen to maintain body temperature. The scalp of a mouse was removed to expose the skull between the bregma and lamda positions. The periosteum of the skull was removed and cleaned thoroughly and dried with air flow for ~20 sec. A thin layer of cryanoacrylate glue was applied to cover the exposed skull. After the mouse head was stereotactically fixed, a closed-head mTBI was produced using a control cortical impact (CCI) device with a modified impactor tip by attaching a 3-mm-diameter round silicone tip of 1.5 mm in thickness on it (Benchmark Stereotaxic Impactor; Leica Impactor One; Meyer Instrument, St. Louis, MO). After the baseline point of the device was set by lowering the tip to the skull surface and stage position was set to zero, the impactor was retracted and impact depth was set. The approximate center of the impact site was 1 mm posterior to the bregma and 0.5 mm lateral from the midline on one cortical hemisphere. The skull was hit with the impactor tip at a speed of 4 m/s to a depth of 2 mm. All animals survived the injury without any skull fracture or hemorrhage.

In vivo *optogenetic mapping of motor cortex*

Optogenetic mapping of bilateral motor cortex was made using a previously described technique.[5] Briefly, mice were anesthetized with a mixture of ketamine (83.85 mg/mL) and xylazine (8.15 mg/mL) and fixed in a stereotaxic frame. This modified mixture of ketamine and xylazine was used for *in vivo* motor mapping because it allowed us to keep the mice in a shallow anesthetic state, but without completely blocking motor response, as the usual concentrations of ketamine and xylazine do. Mice were maintained in an anesthetic level such that they were motionless, but responsive to tail pinch, throughout the course of experiment. An optogenetic mapping setup was used to control the scanning of a 470-nm laser (5 ms duration) on the skull. Each mapping region consisted of a rectangular grid of 5×6 spots with 300-μm spacing between adjacent spots (1.5-by-1.8 mm). Laser pulses were applied onto each spot at a random order until all spots were covered.

Mapping area of each cortical hemisphere consisted of six mapping grids, with a total dimension of $4500 \times 3600 \ \mu$m. Evoked electromyogram (EMG) was recorded with an electrode inserted into anterior biceps brachii of the contralateral forelimb. Signals were amplified using a DP-304 Differential Amplifier (Warner Instrument Corp, Hamden, CT), digitized with a DigiData acquisition system (model 1550B; Molecular Devices, San Jose, CA), and recorded in pClamp 9 (Axon Instruments, Molecular Devices). For each animal, each cortical region was mapped repeatedly three times, and spots with two or three responses were counted as active spots. Spots with zero responses or one response was considered as unresponsive.

EMG responses were detected and analyzed using Detector Analysis software.[5] The amplitude for each stimulated spot was averaged from the amplitudes of two or three repetitions. Numbers of active spots were obtained by counting the spots that produced EMG responses. Average EMG amplitudes with respect to the anterior-to-posterior and medial-to-lateral axes were calculated by averaging all response amplitudes for all active spots along the direction of interest. Motor cortical activity maps were constructed with OriginPro (version 9.1; OriginLab, Northampton, MA).

Cortical slice preparation

GCamp6 mice were anesthetized with 78 mg/kg of ketamine and 22 mg/kg of xylazine (intraperitoneally) and decapitated with scissors. After the scalp was removed, the skull was cut along the midsagittal line, and the two flaps of bone covering both brain hemispheres were removed. The brain was then taken out and immediately placed in an ice-cold 4°C oxygenated sucrose artificial cerebral spinal fluid (s-ACSF) solution (206 mM of sucrose, 2 mM of KCl, 1 mM of $MgCl_2$, 2 mM of $MgSO_4$, 1.25 mM of NaH_2PO_4, 26 mM of $NaHCO_3$, 10 mM of D-glucose, and 1 mM of $CaCl_2$). After 1–2 min, the brain was glued onto a cutting stage such that the cortex faced the approaching blade. A piece of agarose gel was used as a cushion against the ventral part of the brain to prevent movement while cutting. Slices of 350-μm-thick were cut with a Vibratome (Leica VT1200S; Leica, Nusslock, Germany) whereas the brain was submerged in a 4°C cutting solution. Slices were then

incubated at 32°C for 1 h in a gridded chamber filled with oxygenated incubating ACSF (124 mM of NaCl, 3 mM of KCl, 2 mM of MgSO$_4$, 1.25 mM of NaH$_2$PO$_4$, 26 mM of NaHCO$_3$, 10 mM of D-glucose, and 1 mM of CaCl$_2$). Each slice was kept in a grid of the chamber for up to 4 h during an experiment.

Calcium imaging of spontaneous and glutamate uncaging-induced activities of cortical slices

A custom-built recording chamber was made by attaching a temperature-control heated well (Thermal Well Temperature Controller TC-100; BioScience Tools, San Diego, CA) onto a cover-slip. A liquid inflow tubing and a vacuum outflow tubing were installed to generate ACSF circulation through the chamber. A cortical slice was placed in the chamber and secured with a metal ring. Calcium activities of the slice was imaged with a system consisting of a Leica DM6000 FS upright microscope with a Leica EL-6000 120W mercury fluorescence light source directed through a 10× water submerge objective. Videos were captured with an iXON EMCCD DU-88U camera system (Andor USA, Concord, MA). Cortical layers 2 and 3 and layer 5 of the slices were imaged in one of the following conditions: 1) high-potassium ACSF (124 mM of NaCl, 5 mM of KCl, 2 mM of MgSO$_4$, 1.25 mM of NaH$_2$PO$_4$, 26 mM of NaHCO$_3$, 10 mM of D-glucose, and 1 mM of CaCl$_2$); 2) regular ACSF with 20 μM of bicuculline; 3) regular ACSF with 20 μM of bicuculline/20 μM of DNQX; or 4) regular ACSF with 20 μM of bicuculline/50 μM of AP5.

To use glutamate uncaging to evoke neuronal activity in cortical slices, a frequency tripled Nd: YVO$_4$ UV laser (series 3500 pulse laser, $\sim$1 W, 100 KHz repetition rate; DPSS Laser, San Jose, CA) was interfaced with a fiber optic submerged in the slice recording chamber and pointed directly at a cortical area on the slice. A solution of 100 μM of Montreal Neurological Institute–caged glutamate (4-methoxy-7-nitroindolinyl-caged L-glutamate; Toris Bioscience, Minneapolis, MN) in ACSF was used in each experiment. Focal photolysis of caged glutamate was accomplished by switching the UV laser to give a 400- to 800-μs light stimulus.

Analysis of calcium imaging data

Videos of calcium imaging were analyzed *post hoc* using ImageJ software (NIH, Bethesda, MD) with a Time Series Analyzer plugin (Balaji J. UCLA). Only active cells that produced calcium fluorescence flashes at least once during an imaging period were analyzed. For each individual cell, the soma was manually circled, and three separate background regions were chosen by drawing circles of the same diameter in the surrounding area. Selected background areas did not include any dendrites or other neuronal structures. The true calcium fluorescence signal of a cell body or dendrites $\Delta F/F$ was calculated with an equation (Equation 1) excerpted from Chen and colleagues[18] that was developed by Kerlin and colleagues[19]:

$$\frac{\Delta F}{F} = \frac{(F_{true} - F_B)}{F_B} \quad \text{and} \quad F_{true} = F_{cell} - r * F_B \quad (1)$$

where F_B is the baseline fluorescence averaged over three different regions surrounding the cell of interest and r is the contamination ratio standard constant 0.7. These data were then used to construct calcium transient profiles using OriginPro software (version 9.1; OriginLab, Northampton, MA). Peak amplitudes, frequencies, and durations were obtained with a Peak Analysis toolbox of OriginPro 9.1. In short, responding peaks were picked first by setting a minimum response threshold of 20% with respect to the highest amplitude peak of that spectrum. Selected peaks were then compared with its corresponding video to confirm calcium activities. Peak

analysis toolbox then calculated the amplitudes, frequencies, and durations at half maximum height for all events in the spectrum.

Statistical analysis

Final plots were developed in Microsoft Excel (Microsoft Inc., Redmond, WA), and values are reported as mean ± standard error of the mean (SEM). All statistical analyses were done with JMP Analysis (version 11; SAS Institute Inc. 2013; SAS Institute Inc., Cary, NC) and GraphPad Prism (version 6; GraphPad Software, La Jolla, CA). Analysis of variance (ANOVA) analyses were used for comparing numbers of total active spots of optogenetic mapping data (repeated-measures ANOVA), response amplitudes of motor maps (one-way), and amplitudes, frequencies, and durations of calcium imaging data (one-way) and for comparing calcium amplitudes, frequencies, and durations among control, 6,7-dinitroquinoxaline-2,3-dione (DNQX)-, and amino-5-phosphonopentanoate (AP5)-treated groups (two-way). For comparisons that yield statistical significances, Tukey's honestly significant difference (HSD) *post hoc* analyses were applied for further comparisons between specific groups. For glutamate uncaging data, a Pearson's chi-square frequency test was used to compare percentages of active cells among groups at different time points after mTBI.

Results

Mild traumatic brain injury (mTBI) resulted in reduced ipsilateral motor map at 2 h, but enhanced contralateral map at 12 h post-mTBI

We used a CCI device to generate a model of closed-head mTBI in mice. To assess motor functional changes after closed-head mTBI, we utilized optogenetic mapping to monitor potential changes in cortical motor map longitudinally. As a control, we mapped uninjured ChR2-expressing mice at various time points to assess the stability of this technique. In these mice, we found no significant change in the shape and size of maps in 24 h after initial mapping (Fig. 1A), and the numbers of light-responsive spots at 2, 12, and 24 h did not change significantly (Fig. 1B; $p > 0.05$, repeated-measures ANOVA; $n = 7$).

To determine longitudinal changes in cortical motor map after mTBI, recordings of optogenetically evoked EMG responses were made from the same ChR2-expressing mice at baseline and 2, 6, and 12 and 1, 3, and 5 days after injury. We found a significant reduction in numbers of light-responsive spots at 2 h post-injury on the ipsilateral (i.e., ipsilesional) cortex ($\sim$50% reduction vs. baseline; $p < 0.01$, repeated-measures ANOVA; Fig. 2). In contrast, cortical map size on the contralateral cortex did not decrease at 2 h after injury, but was significantly larger at 12 h after injury ($\sim$20% increase vs. baseline; $p < 0.05$, repeated-measures ANOVA; Fig. 2). Cortical maps of both hemispheres returned to baseline level at 72 and 120 h after mTBI (Fig. 2).

We also assessed changes in average amplitudes of evoked EMG events by calculating mean amplitudes at each distance with respect to anterior-to-posterior direction and medial-to-lateral direction (Fig. 3). At 2 h post-mTBI, average EMG amplitudes of ipsilateral forelimb were significantly lower than those of baseline maps (Fig. 3A,B). The lowest average response amplitudes ($\sim$0.2 ± 0.03 mV) were found to be $\sim$1.5 mm lateral and 3.5 mm posterior to the bregma, which correlated to the region surrounding the injury epicenter (Fig. 3A,B; $p < 0.05$, one-way ANOVA). However, we found that average EMG amplitudes of contralateral forelimb at 12 h post-mTBI showed no significant difference compare to those of baseline responses (one-way ANOVA; Fig. 3C,D).
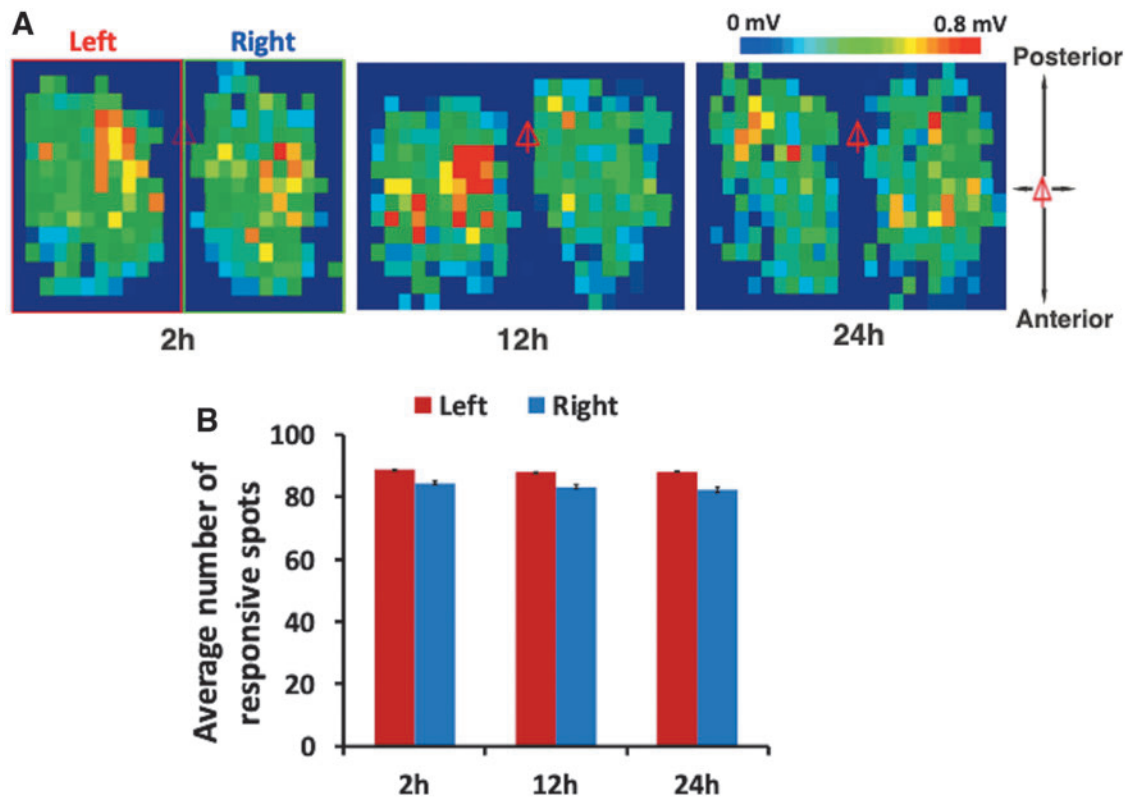
FIG. 1. Repeated optogenetic mapping of motor cortex in a ChR2 mouse produced stable baseline motor maps in 24 h. (**A**) Representative cortical motor maps of both left and right hemispheres from a sham mouse mapped at 2 h, 12 h, and 1 day after skull preparation. Red triangles indicate the position of bregma, and the color bar indicates different peak amplitudes of EMG response. Whereas there existed variabilities in the shape and pattern of motor maps constructed based on EMP peak amplitudes, there were no significant changes in general map size over time. (**B**) There were no significant differences in average numbers of responsive spots in both cortical hemispheres at 2-, 12-, and 24-h mapping times ($n = 7$; mean ± SEM, repeated-measures ANOVA). ANOVA, analysis of variance; EMG, electromyogram; EMP, electromagnetic pulse; SEM, standard error of the mean. Color image is available online.

Calcium imaging of green fluorescent-calmodulin proteins cortical slices revealed decreased ipsilateral calcium signals 2 h after mild traumatic brain injury

To determine whether loss of ipsilateral motor map after mTBI was attributable to reduced cortical neuronal excitability, we used calcium imaging to examine neuronal activity of cortical slices prepared in 2 h post-mTBI from the ipsilateral hemisphere of GCaMP6 transgenic mice. Calcium imaging of cortical slices were done in an ACSF containing 5 mM of potassium chloride to slightly promote neuronal activity for *in vitro* imaging. Comparing to the sham or contralateral cortex, neurons in cortical slices from injured brain usually showed single-, slower-, and lower-amplitude calcium transients (Fig. 4A). They had significantly lower average amplitude of calcium responses than those of sham animals (average $\Delta F/F$ amplitude 0.073 ± 0.015 vs. 0.120 ± 0.010 for 2 h after mTBI group and sham group, respectively; $p < 0.05$, one-way ANOVA; Fig. 4A,B). There was no significant change in peak amplitude on the contralateral cortex (Fig. 4A,B).

There was also a large increase in mean duration of calcium transients of neurons from slices of ipsilateral cortex, but not contralateral (64.9 ± 17.7, 98.3 ± 21.5, and 175.8 ± 12.3 for sham, contralateral, and ipsilateral slices, respectively; $p < 0.05$ for ipsilateral vs. sham groups, one-way ANOVA; Fig. 4A,C), but there were dramatic decreases in frequencies of calcium transients in

both ipsi- and contralateral cortices after mTBI, with neurons of the ipsilateral cortex having more decrease ($\sim 1.00 \pm 0.12$ peaks per cell ipsilateral vs. $\sim 7.0 \pm 1.3$ peaks per cell contralateral vs. ~ 24 peaks per cell sham at 2 h; $p < 0.05$, one-way ANOVA; Fig. 4D). The undercurve area of the ipsilateral cortical neurons was significantly higher than that of the sham group (1.83 ± 0.43 vs. 0.52 ± 0.14 at 2 h for ipsilateral vs. sham; $p < 0.05$, one-way ANOVA; Fig. 4E).

Reduction in α-amino-3-hydroxy-5-methyl-4-isoxazolepropionic acids and N-methyl-D-aspartates calcium signals in cortical slices at 2h after mild traumatic brain injury

We further assessed the contribution of NMDARs and AMPARs to lost activity of the injured cortex. Cortical slices from GCaMP6 mice were first imaged in the presence of 20 μM of bicuculline to reveal spontaneous activities. There were significant decreases in average amplitude and frequency of calcium transients and an increase in calcium duration in the injured slices (Fig. 5). Upon addition of 20 μM of DNQX, there was a significant reduction in signal amplitude in both groups of the control and mTBI groups (0.062 ± 0.006 vs. 0.052 ± 0.009 for before and after DNQX of the control group, respectively, and 0.04 ± 0.007 vs. 0.026 ± 0.004 for before and after DNQX of the mTBI group, respectively; $p < 0.05$,
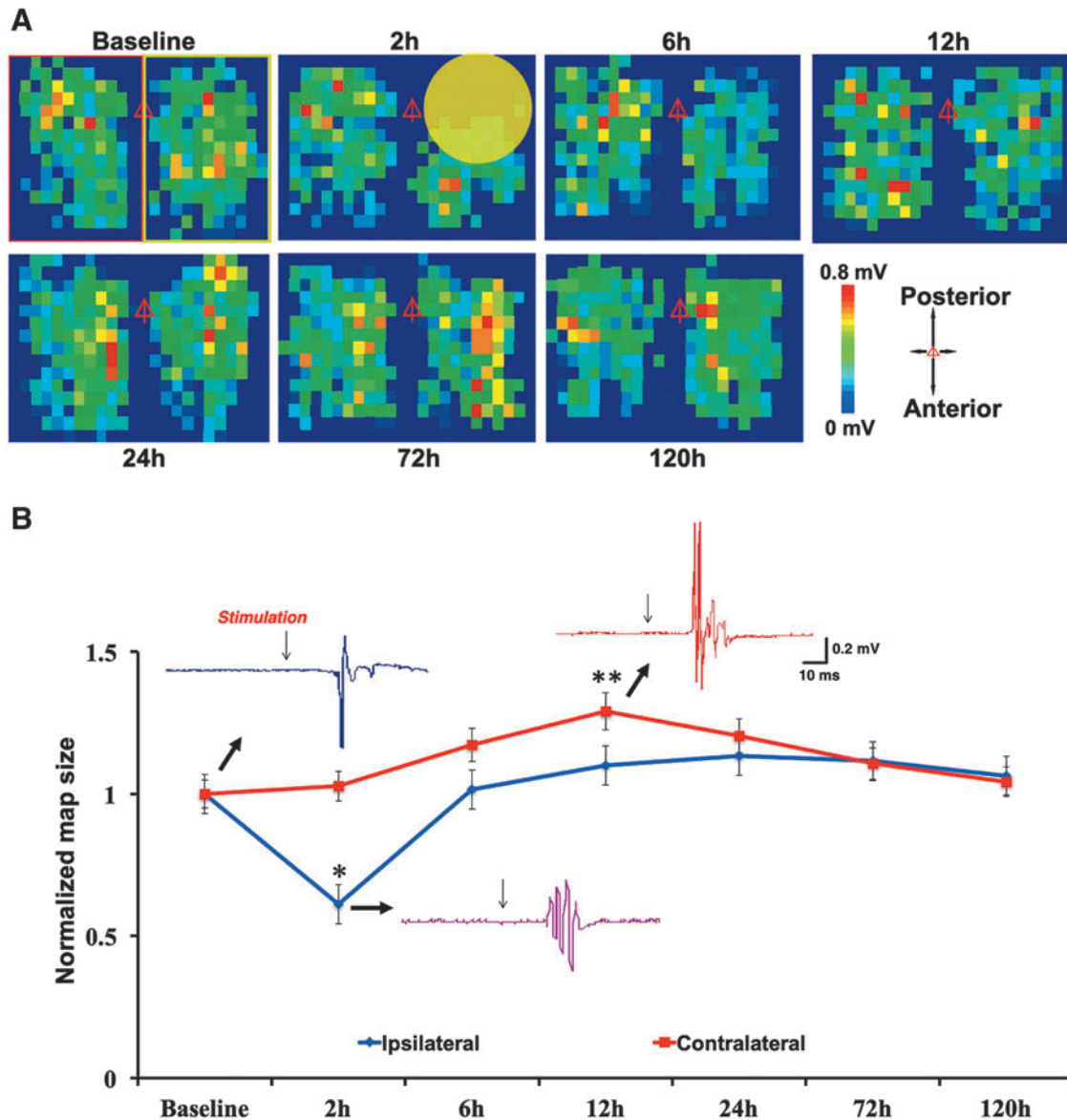
FIG. 2. Optogenetic mapping revealed acute loss of motor map after mTBI followed by recovery of the ipsilateral cortex and transient hyperexcitability of the contralateral cortex. (**A**) Representative motor maps at baseline and different time points after closed-head mTBI. Note loss of motor map at 2 h after mTBI. Red triangles indicate position of bregma, and color bars indicate strength of EMG response. The yellow circle indicates area of impact (~ 3 mm). The green box (right side of map) indicates ipsilateral, and the red box (left side of map) indicates contralateral. (**B**) Mean normalized map size showed that mTBI resulted in a decrease in motor map size (i.e., number of responsive spots) of the ipsilateral cortex at 2 h after injury and recovery at 12 h. In the contralateral cortex, mTBI resulted in a transient increase in map size at 12 h post-injury. Also shown are sample mapping traces of control and post-mTBI EMG responses ($*p < 0.01$; $**p < 0.05$, mean $\pm$ SEM, repeated-measures ANOVA, Turkey's HSD *post hoc*; $n = 7$). ANOVA, analysis of variance; EMG, electromyogram; HSD, honestly significant difference; mTBI, mild traumatic brain injury; SEM, standard error of the mean. Color image is available online.

two-way ANOVA; Fig. 5A,B). However, the injured slices showed a much larger reduction compared to the control group, $\sim 50\%$ reduction (0.026 ± 0.004 of mTBI DNQX vs. 0.052 ± 0.009 of control DNQX; $p < 0.05$, two-way ANOVA). When 50 μM of AP5 was added, an even larger reduction in calcium amplitude occurred in the injured slices, $\sim 60\%$ reduction (0.01 ± 0.004), compared to control slices (0.029 ± 0.003; $p < 0.05$, two-way ANOVA; Fig. 5A,B).

The duration of calcium transients became significantly longer post-mTBI ($\sim 84.8 \pm 6.29$ vs. $\sim 71.2 \pm 5.15$ ms of control) and remained high even with the addition of DNQX (42.8 ± 8.82 vs. 26.6 ± 3.33 ms of control; $p < 0.05$, two-way ANOVA; Fig. 5C). Addition of AP5 produced no noticeable changes. Changes in response frequency of the injured group were similar to those of the response amplitude, with a significant reduction in injured slices ($\sim 3.28 \pm 0.34$ peaks per cell vs. 6.23 ± 1.24 peaks per cell of control; $p < 0.05$, two-way ANOVA) and further reductions after the addition of DNQX or AP5 (1.50 ± 0.69 peaks per cell and 1.06 ± 0.17 peaks per cell of the injury group, respectively, vs. $\sim 2.84 \pm 0.44$ peaks per cell and 1.89 ± 0.25 of the control group, respectively; $p < 0.05$, two-way ANOVA; Fig. 5D).
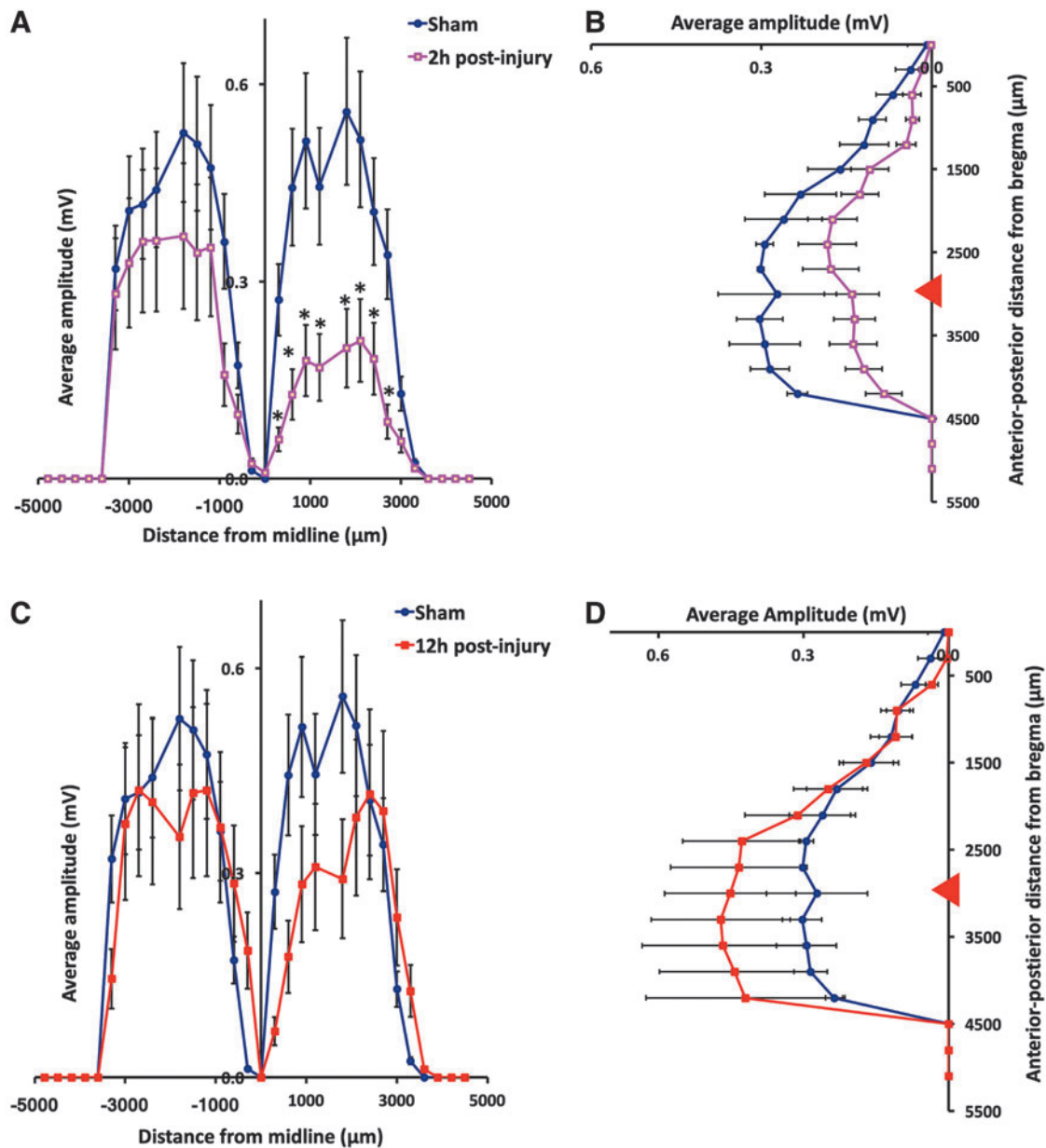
FIG. 3. Decreased ipsilateral response intensity of motor map at 2 h after mTBI. Plots present changes in motor responses along the medial-lateral direction (**A** and **B**) and anterior-posterior direction (**C** and **D**). (A and B) Decreases in light-evoked EMG amplitudes of ipsilateral cortex at 2 h after mTBI (*$p < 0.05$, mean ± SEM, one-way ANOVA, Tukey's HSD; $n = 7$). (C and D) No significant differences in light-evoked EMG amplitudes of contralateral cortex at 12 h after mTBI ($n = 7$; mean ± SEM, one-way ANOVA). Horizontal axis in (A) and (C) presents medial-lateral positions, and vertical axis in (B) and (D) presents posterior-anterior positions. Red triangles in (B) and (D) represent position of bregma. ANOVA, analysis of variance; EMG, electromyogram; HSD, honestly significant difference; mTBI, mild traumatic brain injury; SEM, standard error of the mean. Color image is available online.

Glutamate uncaging of green fluorescent-calmodulin proteins cortical slices revealed reduced calcium signals and impaired α-amino-3-hydroxy-5-methyl-4-isoxazolepropionic acids and N-methyl-D-aspartates function

To directly assess the function of glutamate receptors, we used a glutamate uncaging technique to activate glutamate receptors in cortical slices at multiple time points (Fig. 6). Calcium transients of injured slices at all time points had significant decreases in amplitude compared to sham slices at 2 h after mTBI (0.034 ± 0.002 vs. 0.087 ± 0.010 of sham; $p < 0.05$, one-way ANOVA), 12 h after mTBI (0.030 ± 0.001 vs. 0.087 ± 0.010 of sham), and worsen at 24 h (0.026 ± 0.003 vs. 0.087 ± 0.010 of sham; $p < 0.05$, one-way ANOVA) after mTBI (Fig. 6B). The duration of calcium transient was significantly longer at all time points (244.5 ± 26.9 ms of 2 h, 490.1 ± 89.9 ms of 12 h, and 460.7 ± 78.4 ms of 24 h vs. 99.7 ± 5.93 ms of sham; $p < 0.05$, one-way ANOVA; Fig. 6C).

Further, we noticed gradual increases in the latency period from glutamate uncaging to calcium responses over time after mTBI. In sham slices, 88.3% of responsive neurons had latency periods of <200 ms. After mTBI, only ~69%, 37%, and 28.6% of
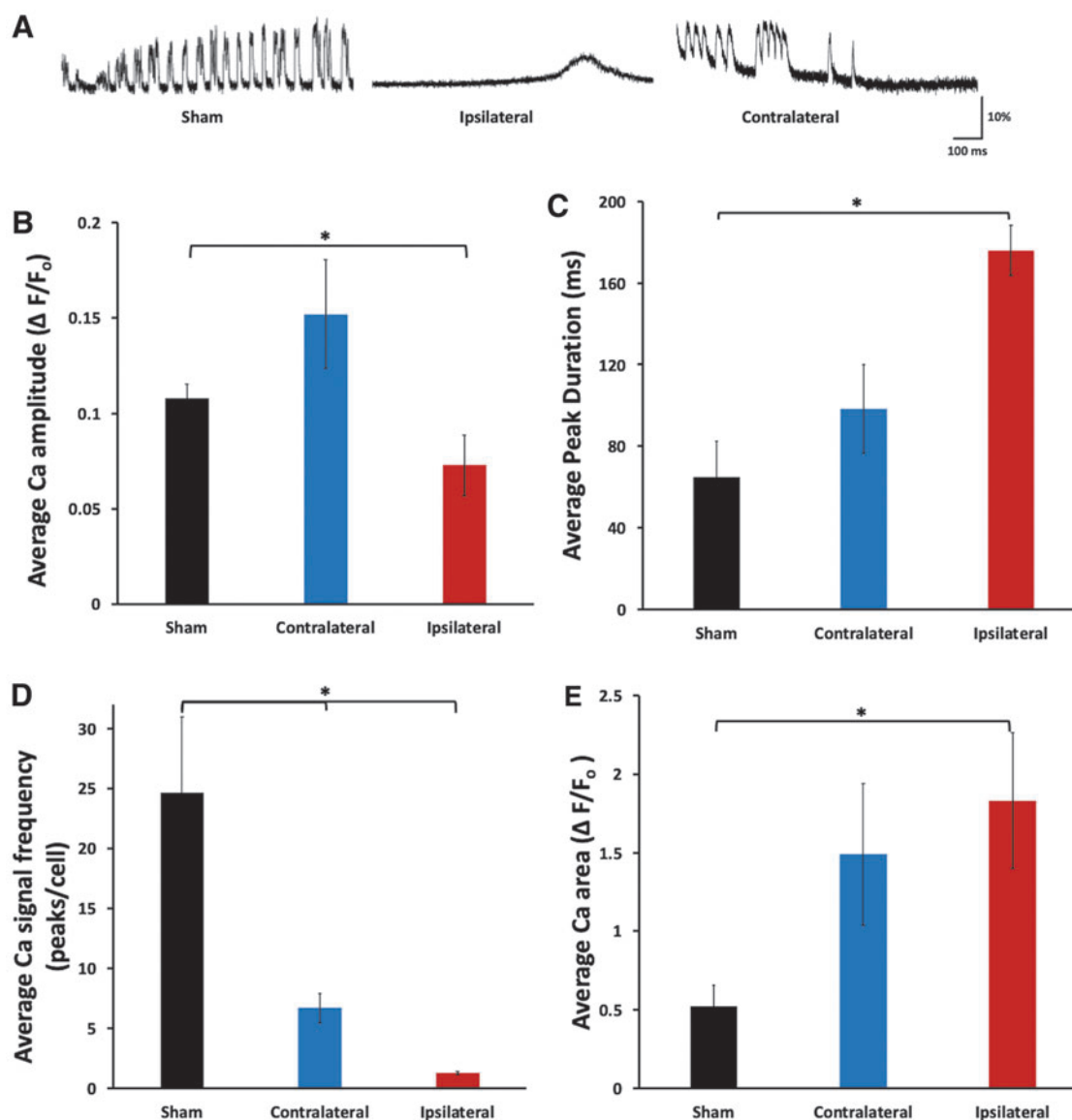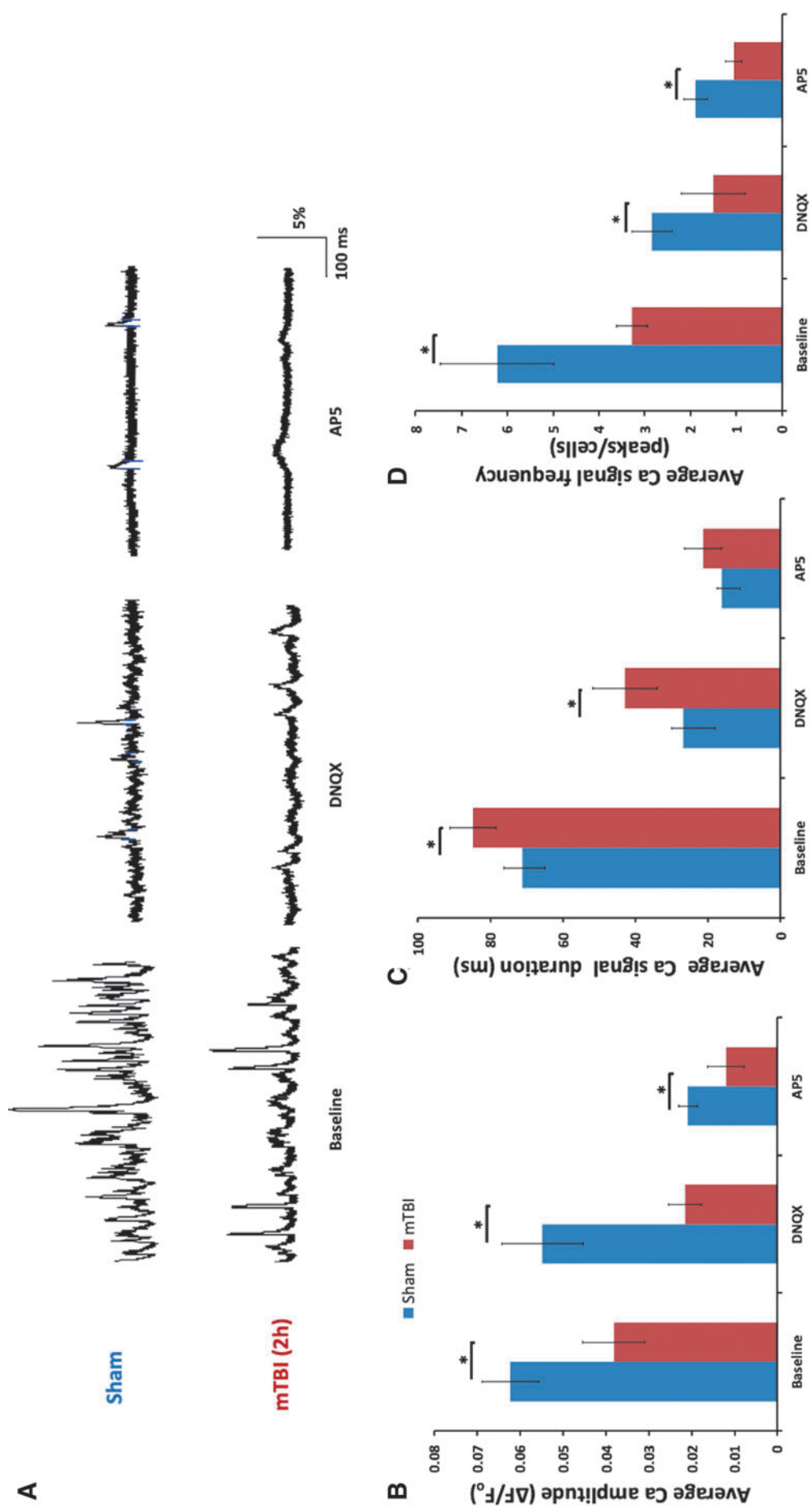
FIG. 4. *Ex vivo* imaging of GCaMP6 cortical slices showed impairments of spontaneous calcium signals on the ipsilateral cortex 2 h after mTBI. (**A**) Examples of spontaneous calcium traces of cortical neurons at baseline and after injury. (**B**) There was a significant reduction in spontaneous calcium peak amplitude of neurons of the ipsilateral cortex, but no significant change in the contralateral cortex, at 2 h after mTBI. (**C**) There was a significant increase in spontaneous calcium peak duration of neurons of the ipsilateral cortex at 2 h after mTBI ($n = 9$ slices per group; $*p < 0.05$, mean ± SEM, one-way ANOVA, Turkey's HSD *post hoc*). (**D**) There were significant decreases in frequencies of spontaneous calcium events of neurons of ipsi- and contralateral cortices at 2 h after mTBI ($n = 9$ slices per group; $*p < 0.05$, mean ± SEM, one-way ANOVA, Turkey's HSD *post hoc*). (**E**) There was a significant increase in the undercurve area of calcium events of ipsilateral cortical neurons at 2 h after mTBI compared to sham ($n = 9$ slices per group; $*p < 0.05$, mean ± SEM, one-way ANOVA, Turkey's HSD *post hoc*). ANOVA, analysis of variance; EMG, electromyogram; GCaMP6, green fluorescent-calmodulin proteins; HSD, honestly significant difference; mTBI, mild traumatic brain injury; SEM, standard error of the mean. Color image is available online.

responsive neurons from the 2-, 12-, and 24-h groups, respectively, had latency periods of <200 ms ($p < 0.001$ for control vs. 2 h, 12 h, and 24 h and $p < 0.05$ for 2 vs. 12 and 24 h; Pearson's chi-square test; Fig. 6D). Consistently, increasingly higher percentages of neurons in later mTBI groups had latency periods between 200 and 500 ms (11.8%, 30.4%, 42.6%, and 64.3% for sham and 2-, 12-, and 24-h groups after mTBI, respectively; $p < 0.001$ for sham vs. 2, 12, and 24 h and $p < 0.05$ for 2 vs. 24 h and 12 vs. 24 h; Pearson's chi-square test; Fig. 6E).

Discussion

Persons who suffer from mTBI exhibit short-term functional deficits in the absence of significant neuronal death and have been observed to recover in the chronic stage.[20–22] Traumatized but surviving neurons may play a role in the functional deficits and recovery of the injured brain. In this study, we have demonstrated that closed-head mTBI in mice caused a transient activity loss of cortical motor map *in vivo*, which is attributable to depressed

FIG. 5. Calcium imaging of GCaMP6 cortical slices showed different losses of AMPA and NMDA receptor signals at 2 h after mTBI. (**A**) Sample traces of spontaneous calcium transients of layer 5 cortical neurons after bicuculline, bicuculline + DNQX, and bicuculline + AP5 treatments. (**B**) There was a significant decrease in calcium peak amplitude at 2 h after mTBI, with larger decreases after application of 50 μM of AP5 in both sham and mTBI slices. (**C**) There were increases in calcium signal duration at 2 h mTBI after mTBI and after application of 20 μM of DNQX in mTBI slices. (**D**) There were significant decreases in calcium signal frequencies at 2 h after mTBI and after application of DNQX or AP5. Scale bar, 400 μm (*$p < 0.05$; mean ± SEM, two-way ANOVA, Turkey's HSD *post hoc*; $n = 8$ slices per group). AMPA, α-amino-3-hydroxy-5-methyl-4-isoxazolepropionic acid; ANOVA, analysis of variance; AP5, amino-5-phosphonopentanoate; DNQX, 6,7-dinitroquinoxaline-2,3-dione; EMG, electromyogram; GCaMP6, green fluorescent-calmodulin proteins; HSD, honestly significant difference; mTBI, mild traumatic brain injury; NMDA, N-methyl-D-aspartate; SEM, standard error of the mean. Color image is available online.
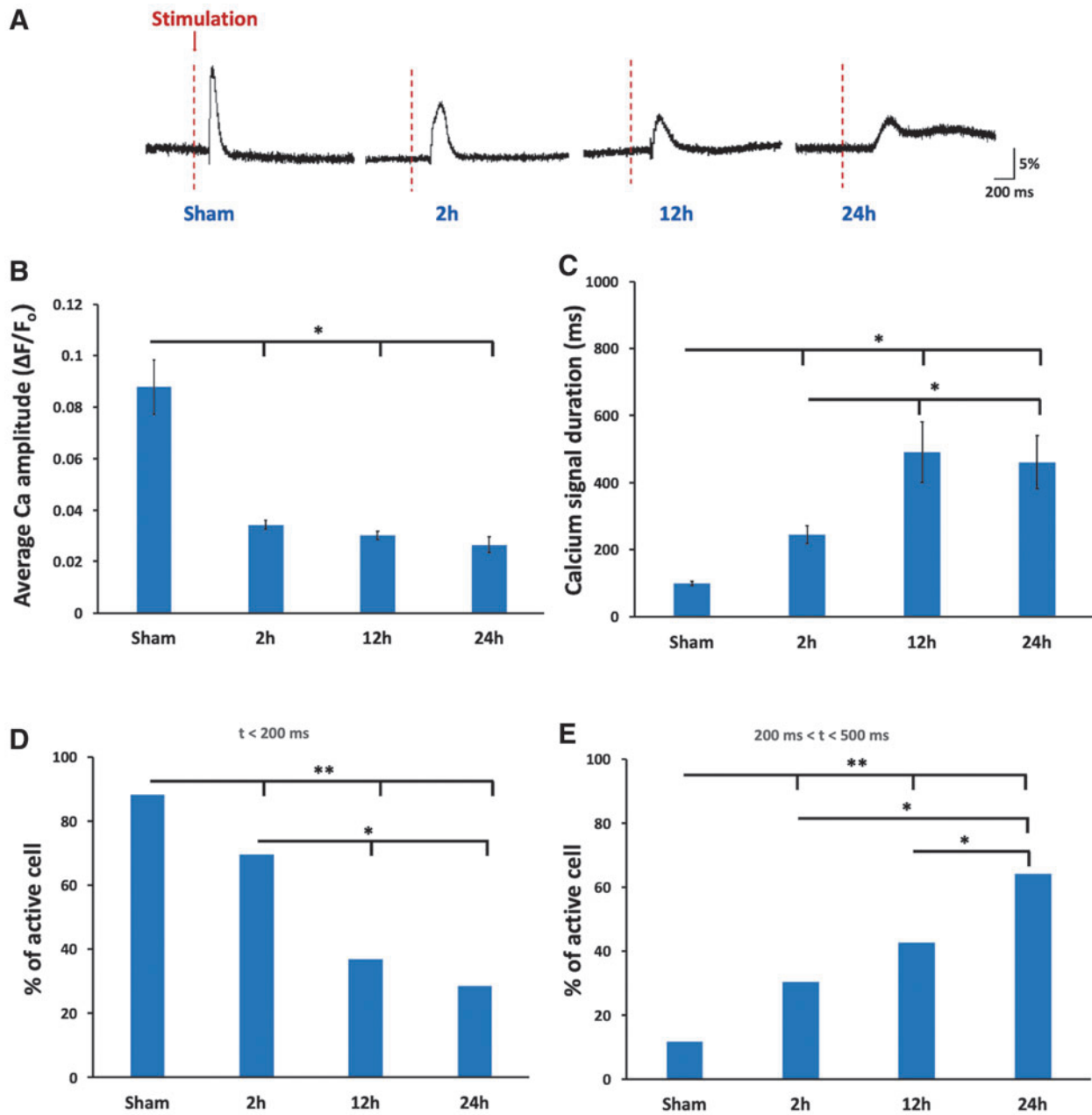
FIG. 6. Glutamate uncaging in GCaMP6 cortical slices revealed reduced calcium signals with longer latency at 2 h after mTBI. (**A**) Sample traces of calcium responses in slices evoked by glutamate uncaging at baseline, 2, 12, and 24 h after mTBI. (**B**) mTBI resulted in significantly decreased calcium signal amplitudes at 2, 12, and 24 h after injury. (**C**) mTBI resulted in significantly increased calcium signal duration at 2, 12, and 24 h after injury ($*p < 0.05$, mean ± SEM, one-way ANOVA, Tukey's HSD; $n = 11$ slices per group). (**D**) Percentages of neurons with response latency <200 ms became increasingly decreased at 2, 12, and 24 h after injury. (**E**) Percentages of neurons with response latency between 200 and 500 ms became increasingly larger at 2, 12, and 24 h after mTBI. ($**p < 0.001$; $*p < 0.05$, mean ± SEM, Pearson's chi-square test). ANOVA, analysis of variance; GCaMP6, green fluorescent-calmodulin proteins; HSD, honestly significant difference; mTBI, mild traumatic brain injury; SEM, standard error of the mean. Color image is available online.

cortical neuronal activity attributable to impaired NMDA and AMPA receptor functions and calcium homeostasis.

This study is the first study to use a repeated *in vivo* optogenetic motor mapping technique as a functional readout to evaluate longitudinal changes in motor function after mTBI. This highly efficient technique provides a reproducible and minimally invasive approach for generating functional maps to obtain insights into the electrophysiological properties and longitudinal changes of the corticospinal pathway.[4–6] Using this novel approach, we found that mTBI resulted in a significant loss in cortical motor map in 2 h after trauma. This result is consistent with previous behavioral findings in animals showing loss of righting reflex up to at least 2 h after injury[23] and impaired motor function during the rotarod test for up to 1 day.[24] Our results also support previous findings in concussion

patients who were shown to suffer an increased cortical silence period, indicative of long-term intracortical inhibition[25] and in football athletes who sustained concussions performed significantly worse in dexterity, reaction, and movement tests.[26] Interestingly, the motor map of the uninjured contralateral hemisphere had a significant increase in map size in 12 h post-mTBI. This suggests there may be a compensatory mechanism in response to the hypoactivity of the injured cortex.

Our *in vivo* longitudinal mapping results confirm that closed-head mTBI induces hypoexcitability of the injured cortex. In contrast, there have been many reports of hyperexcitability in the acute phase of TBI attributable to increased release of glutamate and excitotoxicity that may cause subsequence loss of cortical function.[27,28] However, the increase in extracellular glutamate is transient, lasting from only a few minutes in mTBI[10] to 0.5 h in more severe TBI.[9] Several clinical trials, such as the selfotel trials in particular, were undertaken to block neuronal hyperexcitability with different glutamate receptor antagonists, but the results were inconsistent, with some of them even showing detrimental effects.[14,15,29] In contrast, several studies found that expression of ionotropic glutamate receptors, including NMDA receptors[11,30] and AMPARs,[13] actually decrease after brain injury. Loss of these receptor expressions peaks during the first 24 h post-injury and lasts for 7 days.[12,31,32] Further, these losses could be attributed to reduction in surface expression of NMDA receptor subunits NR1/NR2A/NR2B,[33] AMPA receptor subunit glutamate receptor 1,[34] and downregulations of receptor synthesis.[32] Consistently, activating AMPA or NMDA receptors during the acute phase after injury improves functional outcomes of animals with a wide range of TBI severities.[11,35]

Given that calcium is a major intracellular signaling molecule in neurons, alterations in calcium homeostasis could have significant effects on neuronal physiology and network activity. Therefore, the assessment of glutamate receptor function, a major contributor to neuronal calcium transient, is an important step in understanding how brain activity changes after trauma. Using *in vitro* imaging of cortical slices from GCaMP6 transgenic mice, we showed a loss in spontaneous cortical neuronal calcium signals shortly after injury and this loss occurred mainly in the injured hemisphere, but not in the contralateral hemisphere, 2 h after injury. This is consistent with recent evidence of reduced calcium dynamics during the acute phase in a blast brain injury model.[36] An increase in the duration of calcium transients in the injured cortex points to a longer retention of Ca^{2+} in the cytosol. This change in intracellular Ca^{2+} clearance may be a compensatory mechanism or, more likely, an impairment in calcium regulation between the cytosol and extracellular space or with intracellular calcium storage (i.e., endoplasmic reticulum [ER] and mitochondria).

Earlier studies in hippocampal CA3 neurons after a fluid percussion TBI have shown that prolonged retention of Ca^{2+} in the cytosol could be attributable to impaired calcium clearance.[22,37] This cytosolic calcium dysregulation after TBI could be attributed to impairments in calcium buffering capacity, neuronal membrane Na/Ca exchanger, and intracellular ER/mitochondria storage.[38,39] For example, mechanically induced injury has been shown to alter mitochondrial membrane potential and reduce ATP levels in neurons in the absence of hypoxia.[40,41] A reduction in ATP severely affects the role of sarcoplasmic/endoplasmic reticulum calcium ATPase (SERCA) and plasma membrane calcium ATPase (PMCA) in pumping Ca^{2+} either into storage (ER/mitochondria) or extracellular space and results in Ca^{2+} accumulations for longer time in the cytosol.[40,42] When blocking NMDA receptors with AP5

to assess AMPAR-dominant calcium transient, we found an almost 60% reduction in calcium transient compared to $\sim$50% by DNQX. This indicates that the majority of calcium influx from the extracellular space occurs through NMDAR receptors and that NMDAR impairment may be responsible for the majority of signal decline in mTBI-induced loss of calcium signals.

Our results are consistent with an earlier report of a 20–40% loss in NMDA receptor expressions in cortex hippocampus 5 min to up to 24 h after fluid percussion induced–TBI.[12] Further, they also found that AMPA receptor expression level was reduced at a similar level ($\sim$25% loss from baseline) from 5 min up to 3 h after trauma, but recovered to a normal level in 24 h. Future investigation using whole-cell patch clamp recordings may provide more precise measurements of changes in AMPA- and NMDA-receptor function after mTBI.

Use of the glutamate uncaging technique allowed us to directly test changes in the function of major glutamatergic calcium channels of NMDAR and AMPAR after mTBI. These glutamate-derived calcium influxes were reduced at 2 h and subsequently remained low up to 24 h after trauma. In addition, calcium signals in response to glutamate uncaging were dramatically altered, with faster responses being increasingly replaced by slower ones at later time points post-mTBI. This further suggests that impairment of glutamatergic ion channels such as NMDAR and AMPAR persist long after mTBI. This longer-lasting impairment of NMDAR could contribute to long-term synaptic dysfunction. Given that impairment in NMDA receptors lasted for a longer time period, functional recovery of the *in vivo* motor maps could be attributed to reduction of cortical inhibition[43] and recovery of other glutamate receptors, such as AMPARs,[44] which may increase the influx of Na^+ into cells to cause membrane depolarization.[45]

Although functional changes after mTBI are often transient and followed by functional recovery at a later time point, understanding these early changes after a single mild injury may help us to understand changes after repeated and more severe injuries. Similar to spontaneous calcium signals, the duration of calcium signals evoked by glutamate uncaging became longer for all time points after mTBI. Although current data do not answer which factors contribute to changes in cytosolic calcium signal, intracellular calcium channels, such as ryanodine receptors, SERCA pumps of ER, and calcium uniporters of mitochondria, may play a potential role in regulating intracellular calcium post-mTBI.[42,46,47] Interestingly, prolonged elevations and retention of intracellular calcium, though not leading to neuronal death, have been demonstrated to cause alterations in neuronal excitability[48,49] and long-term changes in gene expression[50,51] even during the acute phases of TBI.[52–54]

As the most common form of brain trauma, mTBI can produce acute and transient effects, which may subsequently contribute to long-lasting sequelae, especially in cases where multiple mTBI occurs over a short period of time. Using a combination of *in vivo* optogenetic motor mapping, activity imaging in cortical slices from GCaMP6 transgenic mice, and glutamate uncaging, this study demonstrates a transient deficit in the function of motor cortex *in vivo* after mTBI and the contribution of impaired glutamate receptor function. With our novel approach to mTBI using optogenetic mapping, our study shows that mTBI induced short-term neuronal *hypo*excitability in the injured cortex, as indicated by the loss of motor maps and the smaller and longer-lasting calcium transients. We also found that the impairments in calcium signals were attributable to a reduction in the activities of NMDA receptors and AMPA receptors and impaired intracellular calcium homeostasis.

A deeper understanding of the mechanisms that alter neuronal calcium homeostasis in the injured brain may offer novel therapeutic strategies to effectively relieve morbidities associated with mTBI.

Author Disclosure Statement

No competing financial interests exist.

References

1. Roozenbeek, B., Maas, A.I., and Menon, D.K. (2013). Changing patterns in the epidemiology of traumatic brain injury. Nat. Rev. Neurol. 9, 231–236.
2. Povlishock, J.T., and Katz. D.T. (2005). Update of neuropathology and neurological recovery after traumatic brain injury. J. Head Trauma Rehabil. 20, 76–94.
3. Graham, D.T., McIntosh, T.K., Maxwell, W.L., and Nicoll, J.A. (2000). Recent advances in neurotrauma. J. Neuropathol. Exp. Neurol. 59, 641–651.
4. Ayling, O.G.S., Harrison, T.C., Boyd, J.D., Goroshkov, A., and Murphy, T.H. (2009). Automated light-based mapping of motor cortex by photoactivation of channelrhodopsin-2 transgenic mice. Nat. Methods 6, 219–224.
5. Qian, J., Wu, W., Xiong, W., Chai, Z., Xu, X.M., and Jin, X. (2019). Longitudinal optogenetic motor mapping revealed structural and functional impairments and enhanced corticorubral projection after contusive spinal cord injury in mice. J. Neurotrauma 36, 485–499.
6. Omlor, W., Wahl, A.-S., Sipila, P., Lutcke, H., Laurenczy, B., Chen, I.W., Sumanovski, LT., van't-Hoff, M., Bethge, P., Voigt, F.F., Schwab, M.E., and Helmchen, F. (2019). Context-dependent limb movement encoding in neuronal populations of motor cortex. Nat. Commun. 10, 4812.
7. Arundine, M., and Tymianski, M. (2004). Molecular mechanisms of glutamate-dependent neurodegeneration in ischemia and traumatic brain injury. Cell Mol. Life Sci. 61, 657–668.
8. Yi, J.H., and Hazell, A.S. (2006). Excitotoxic mechanisms and the role of astrocytic glutamate transporters in traumatic brain injury. Neurochem. Int. 48, 394–403.
9. Faden, A.I., Demediuk, P., Panter, S.S., and Vink, R. (1989). The role of excitatory amino acids and NMDA receptors intraumatic brain injury. Science 244, 394–403.
10. Nilsson, P., Ronne-Engström, E., Flink, R., Ungerstedt, U., Carlson, H., and Hillered, L. (1994). Epileptic seizure activity in the acute phase following cortical impact trauma in rat (glutamate level post TBI). Brain Res. 637, 227–232.
11. Biegon, A., Fry, P.A., Paden, C.M., Alexandrovich, A., Tsenter, J., and Shohami, E. (2004). Dynamic changes in N-methyl-D-aspartate receptors after closed head injury in mice: Implications for treatment of neurological and cognitive deficits. Proc. Natl. Acad. Sci. U. S. A. 101, 5117–5122.
12. Miller, L.P., Lyeth, B.G., Jenkins, L.W., Oleniak, L., Panchision, D., Hamm, R.J., Phillips, L.L., Dixon, C.E., Clifton, G.L., and Hayes, R.L. (1990). Excitatory amino acid receptor subtype binding following traumatic brain injury. Brain Res. 526, 103–107.
13. Goforth, P.B., Ren, J., Schwartz, B.S., and Satin, L.S. (2011). Excitatory synaptic transmission and network activity are depressed following mechanical injury in cortical neurons. J. Neurophysiol. 105, 2350–2363.
14. Ikonomidou, C., and Tursky, L. (2002). Why did NMDA receptor antagonists fail clinical trials for stroke and traumatic brain injury? Lancet Neurol. 1, 383–386.
15. Morris, G., Bullock, R., Marshal, S., Marmarou, A., Maas, A., and Marshall, L. (1999). Failure of competitive N-methyl-D-aspartate antagonist Selfotel (CGS 19755) in the treatment of severe head injury: results of two phase III clinical trials. J. Neurosurg. 91, 737–743.
16. Creed, J.A., DiLeonardi, A.M., Fox, D.P., Tessler, A.R., and Raghupathi, R. (2011). Concussive brain trauma in the mouse results in acute cognitive deficits and sustained impairment of axonal function. J. Neurotrauma 28, 547–563.
17. Han, X., Chai, Z., Ping, X., Song, L., Ma, C., Ruan, Y., and Jin X. (2020). In vivo two-photon imaging reveals acute cerebral vascular spasm and microthrombosis after mild traumatic brain injury in mice. Front. Neurosci. 14, 210.
18. Chen, T.-W., Wardill, T.J., Sun, Y., Pulver, S.R., Renninger, S.L., Baohan, A., Schreiter, E.R., Kerr, R.A., Orger, M.B., Jayaraman, V., Looger, L.L. Svoboda, K., and Kim, D.S. (2013). Ultrasensitive fluorescent proteins for imaging neuronal activity. Nature 499, 295–300.
19. Kerlin, A., Andermann, M.L., Berezovskii, V., and Reid, R.C. (2010). Broadly tuned response properties of diverse inhibitory neuron subtypes in mouse visual cortex. Neuron 67, 858–871.
20. Delahunty, T.M., Jiang, J.Y., Gong, Q.Z., Black, R.T., and Lyeth, B.G. (1995). Differential consequences of lateral and central fluid percussion brain injury on receptor coupling in rat hippocampus. J. Neurotrauma 12, 1045–1057.
21. Zohar, O., Rubovitch, V., Milman, A., Schreiber, S., and Pick, C.G. (2011). Behavioral consequences of minimal traumatic brain injury in mice. Acta Neurobiol. Exp. (Wars.) 71, 36–45.
22. Sun, D.A., Deshpande, L.S., Sombati, S., Baranova, A., Wilson, M.S., Hamm, R.J., and DeLorenzo, R.J. (2008). Traumatic brain injury causes a long-lasting calcium Ca plateau of elevated intracellular Ca levels and altered Ca homeostatic mechanisms in hippocampal neurons surviving traumatic brain injury. Eur. J. Neurosci. 27, 1659–1672.
23. Antal, J., d'Amore, A., Nerozzi, D., Palazzesi, S., Pezzini, G., and Loizzo, A. (1992). An EEG analysis of drug effects after mild head injury in mice. Life Sci. 51, 185–193.
24. Chen, Y.C., Mao, H., Yang, K.H., Abel, T., and Meaney, D.F. (2014). A modified controlled cortical impact technique to model mild traumatic brain injury mechanics in mice. Front. Neurol. 5, 100.
25. Miller, N.R., Yasen, A.L., Maynard, L.F., Chou, L.-S., Howell, D.R., and Christie, A.D. (2014). Acute and longitudinal changes in motor cortex function following mild traumatic brain injury. Brain Inj. 28, 1270–1276.
26. Pearce, A.J., Hoy, K., Rogers, M.A., Corp, D.T., Maller, J.J., Drury, H.G.K., and Fitzgerald, P.B. (2014). The long-term effects of sports concussion on retired Australian football players: a study using transcranial magnetic stimulation. J. Neurotrauma 31, 1139–1145.
27. Dixon, C.E., Taft, W.C., and Hayes, R.L. (1993). Mechanisms of mild traumatic brain injury. J. Head Trauma Rehabil. journals.lww.com/head traumarehab/Abstract/1993/09000/Mechanisms_of_mild_traumatic_ brain_injury.3.aspx (Last accessed December 26, 2020).
28. Spaethling, J.M., Klein, D.M., Singh, P., and Meaney, D.F. (2008). Calcium-permeable AMPA receptors appear in cortical neurons after traumatic mechanical injury and contribute to neuronal fate. J. Neurotrauma 25, 1207–1216.
29. Farin, A., and Marshall, L.F. (2004). Lessons from epidemiologic studies in clinical trials of traumatic brain injury. Acta Neurochirurg. Suppl. 89, 101–107.
30. Grossman, R., Shohami, E., Alexandrovich, A., Yatsiv, I., Kloog, Y., and Biegon, A. (2003). Increase in peripheral benzodiazepine receptors and loss of glutamate NMDA receptors in a mouse model of closed head injury: a quantitative autoradiographic study. Neuroimage 20, 1971–1981.
31. Sihver, S., Marklund, N., Hillered, L., Langstrom, B., Watanabe, Y., and Bergstrom, M. (2001). Changes in mACh, NMDA and GABA(A) receptor binding after lateral fluid-percussion injury: in vitro autoradiography of rat brain frozen sections. J. Neurochem. 78, 417–423.
32. Friedman, L.K., Ginsberg, M.D., Belayv, L., Busto, R., Alonso, O.F., Lin, B., and Globus, M.Y. (2001). Intra-ischemic but not postischemic hypothermia prevents non-selective hippocampal downregulation of AMPA and NMDA receptor gene expression after global ischemia. Brain Res. 86, 34–47.
33. Kumar, A., Zou, L., Yuan, X., Long, Y., and Yang, K. (2002). N-methyl-D-aspartate receptors: transient loss of NR1/NR2A/NR2B subunits after traumatic brain injury in a rodent model. J. Neurosci. Res. 67, 781–786.

34. Schumann, J., Alexandrovich, G.A., Biegon, A., and Yaka, R. (2008). Inhibition of NR2B phosphorylation restores alterations in NMDA receptor expression and improves functional recovery following traumatic brain injury in mice. J. Neurotrauma 25, 945–957.

35. Ikonomidou, C., Stefovska, V., and Turski, L. (2000). Neuronal death enhanced by N-methyl-D-aspartate antagonists. Proc. Natl. Acad. Sci. U. S. A. 97, 12885–12890.

36. Hansen, K., DeWalt, G.J., Mohammed, A., Tseng, H., Abdulkerim, M., Bensussen, S., Saligrama, V., Nazer, B., Eldred, W., and Han, X. (2018). Mild blast injury produces acute changes in basal intracellular calcium levels and activity patterns in mouse hippocampal neurons. J. Neurotrauma 35, 1523–1536.

37. Slemmer, J.E., Shacka, J.J., Sweeney, M.I., and Weber, J.T. (2008). Antioxidants and free radical scavengers for the treatment of stroke, traumatic brain injury and aging. Curr. Med. Chem. 15, 404–414.

38. Brittain, M., Tatiana Brustovetsky, T., and Brutovesky, N. (2013). Delayed calcium dysregulation in neurons requires both the NMDA receptor and the reverse Na/Ca exchanger. Neurobiol. Dis. 46, 109–117.

39. Weber, J., Rzigalinski, B.A., and Ellis, E. (2000). Traumatic injury of cortical neurons causes changes in intracellular calcium stores and capacitative calcium influx. J. Biol. Chem. 276, 1800–1807.

40. Tavalin, S.J., Ellis, E.F., and Satin, L.S. (1997). Inhibition of the electrogenic Na pump underlies delayed depolarization of cortical neurons after mechanical injury or glutamate. J. Neurophysiol. 77, 632–638.

41. Ahmed, S.M., Weber, J.T., Liang, S., Willoughby, K.A., Sitterding, H.A., Rzigalinski, B.A., and Ellis, E.F. (2002). NMDA receptor activation contributes to a portion of the decreased mitochondrial membrane potential and elevated intracellular free calcium in strain-injured neurons. J. Neurotrauma 19, 1619–1629.

42. Parsons, J.T., Churn, S.B., and DeLorenzo, R.J. (1997). Ischemia-induced inhibition of calcium uptake into rat brain microsomes mediated by Mg^{2+}/Ca^{2+} ATPase. J. Neurochem. 68, 1124–1134.

43. Hsieh, T.H., Cheong Lee, H.H., Hameed, M.Q., Pascual-Leone, A., Hensch, T.K., and Rotenberg, A. (2017). Trajectory of parvalbumin cell impairment and loss of cortical inhibition in traumatic brain injury. Cereb. Cortex 27, 5509–5524.

44. Goforth, P.D.,Ellis, E.F., and Satin, L.S. (2004). Mechanical injury modulates AMPA receptor kinetics via an NMDA receptor-dependent pathway. J. Neurotrauma 21, 719–732.

45. Wolf, J.A., Stys, P.K., Lusardi, T., Meaney, D., and Smith, D.H. (2001). Traumatic axonal injury induces calcium influx modulated by tetrodotoxin-sensitive sodium channels. J. Neurosci. 21, 1923–1930.

46. Weber, J. (2012). Altered calcium signaling following traumatic brain injury. Front. Pharmacol. 3, 60.

47. Limbrick, D.D., Jr., Pal, S., and DeLorenzo, R.J. (2001). Hippocampal neurons exhibit both persisten Ca influx and impairment of Ca sequestration/extrusion mechanisms following 21 excitotoxic glutamate exposure. Brain Res. 894, 56–67.

48. Sun, D.A., Sombati, S., Blair, R.E., and Delorenzo, R.J. (2002). Calcium dependent epileptogeneiss in an in vitro model of stroke-induced epilepsy. Epilepsia 43, 1296–1305.

49. Delorenzo, R.J., Sun, D.A., and Deshpande, L.S. (2005). Cellular mechanisms underlying acquired epilepsy: the calcium hypothesis of the induction and maintenance of epilepsy. Pharmacol. Ther. 105, 229–266.

50. Morris, T.A., Jafari, N., Rice, A.C., Vasconcelos, O., and DeLorenzo, R.J. (1999). Persistent increased DNA-binding and expression of serum response facgtor occur with epilepsy-associated long-term plasticity changes. J. Neurosci. 19, 8234–8243.

51. Morris, T.A., Jafari, N., and DeLorenzo, R.J. (2000). Chronic deltaFos B expression and increased Ap-1 transcription factor binding are associated with long term plasticity changes in epilepsy. Brain Res. Mol. Brain Res. 79, 138–149.

52. Hayes, R.L., Yang, K., Raghupathi, R., and McIntosh, T.K. (1995). Changes in gene expression following traumatic brain injury in rat. J. Neurotrauma 12, 779–790.

53. Raghupathi, R., and McIntosh, T.K. (1996). Regionally and temporally distinct patterns of induction of c-fos, c-jun and junB mRNAs following experimental brain injury in rat. Brain Res. 37, 134–144.

54. Morrison, B., Eberwine, J.H., Meaney, D.F., and McIntosh, T.K., (2000). Traumatic injury induces differential expression of cell death genes in organotypic brain slice cultures determined by complementary DNA array hybridization. Neuroscience 96, 131–139.

Address correspondence to:
Xiaoming Jin, PhD
Indiana Spinal Cord and Brain Injury Research Group
Stark Neuroscience Research Institute
and Department of Anatomy, Cell Biology, and Physiology
Indiana University School of Medicine
320 West 15th Street, NB 500C
Indianapolis, IN 46202
USA

E-mail: xijin@iupui.edu